BUTTERWORTH
HEINEMANN

Roles of pressure transport and intermittency for computation of turbulent free shear flows

Soong Kee Kim* and Myung Kyoon Chung
Department of Mechanical Engineering, Korea Advanced Institute of Science and Technology, Yusong, Taejon, Korea

A Reynolds stress model that includes the recent models of the pressure transport term and the intermittency interaction term is applied to compute various free shear flows. The test computations reveal favorable improvements by the pressure transport model near the free-stream edges of the free shear flows. Inclusion of an intermittency interaction term in the dissipation rate equation also significantly enhances the prediction capability of the Reynolds stress model. In particular, predictions of the Reynolds stresses in the high-velocity side of a plane mixing layer and in the outer layer of a plane wake are remarkably improved.

Keywords: Reynolds stress model; pressure transport; turbulence; free shear flow

Introduction

Recent research efforts on the development of Reynolds stress models have focused mainly on refining the pressure–strain correlation model. Typical are those of Shih and Lumley (1985), Haworth and Pope (1986), Fu, Launder, and Tselepidakis (1987), Shih, Mansour, and Chen (1987), and Speziale, Sarkar, and Gatski (1991, hereinafter referred to as SSG). With such long and extensive researchers, however, the current Reynolds stress models fail to predict simple free shear flows. For example, when the model constants of the Reynolds stress equation are adjusted to yield correct spread rate of a two-dimensional (2-D) jet, then the Reynolds stress model underpredicts the spread rate of a 2-D far wake by as much as 30% (see 1980–81 Stanford Conference).

One of the main reasons for this is the neglect of the pressure transport term in the current Reynolds stress equation. In fact, in a recent review paper, Bradshaw (1994) inferred that the pressure transport plays a significant role near the freestream edges of mixing layers and jets where pressure fluctuations, generated in the high-intensity region of the flow, drive an irrotational motion that extends outside the vortical region. Quite recently, we have developed a new pressure transport model based on the Euler equation and both experimental and DNS data (Kim and Chung 1994). The model consists of a bulk convective transport term and a counter diffusive term.

Another reason for the aforementioned failure is caused by the intermittent nature of turbulence in the free boundary regions. Cho and Chung (1992) found that, depending upon the entrainment direction, the local intermittency factor either increases or decreases, which results in variation of the eddy viscosity. They proposed to modify the standard dissipation equation to include an intermittency invariant term Γ, which represents the entrainment of irrotational fluid into rotational one or vice versa by an interaction between the mean velocity gradient and the intermittency field. Their k-ε-γ model has proved most effective in obtaining correct spreading rates of various kinds of free shear flows.

The main objective of this study is to test the performance of our pressure transport model against free shear flows. Another objective is to extend Cho and Chung's (1992) concept of the intermittency interaction to the Reynolds stress model. To choose a basic reference Renolds stress model for the present comparative study, two diffusion models of Hanjalic and Launder (1972, hereinafter referred to as HL) and Mellor and Herring (1973, hereinafter referred to as MH) and two pressure strain models of Launder, Reece, and Rodi (1975, hereinafter referred to as LRR) and SSG are first tested by computing simple free shear flows; i.e., a plane mixing layer, a plane jet, and a plane far wake. After this comparison test, the basic reference Reynolds stress model is composed of HL's diffusion model and SSG's pressure strain model. Then the second and third sets are constructed by successively introducing the intermittency model of Cho and Chung (1992) and the pressure transport model of Kim and Chung (1994) into the basic reference set. Such strategy makes it convenient to isolate the improvement by each modification in the modeling accuracy. Computational results and some discussion about the roles of the pressure transport and the intermittency in the free shear flows are given in the final part of the paper.

Address reprint request to Professor M. K. Chung, Department of Mechanical Engineering, KAIST, Yusong, Taijon, 305-701, South Korea.

* Present address: Automotive Technology Laboratory, Institute for Advanced Engineering, 541, 5-ga Namdemun-no, Chung-gu, Seoul, 100-714, Korea.

Received 30 August 1994; accepted 3 February 1995.

Int. J. Heat and Fluid Flow 16: 194–201, 1995

0142-727X/95/$10.00
SSDI 0142-727X(95)00011-E

Reynolds stress model

Reynolds stress equation

An exact equation describing the transport of the Reynolds stress $\overline{u_i u_j}$ for an isothermal incompressible flow can be written in the following form:

$$\frac{d\overline{u_i u_j}}{dt} = -\left[\overline{u_j u_k}\frac{\partial U_i}{\partial x_k} + \overline{u_i u_k}\frac{\partial U_j}{\partial x_k}\right] - 2\nu\overline{\frac{\partial u_i}{\partial x_k}\frac{\partial u_j}{\partial x_k}} - \frac{1}{\rho}\overline{\left(u_i\frac{\partial p}{\partial x_j} + u_j\frac{\partial p}{\partial x_i}\right)} - \frac{\partial}{\partial x_k}\left[\overline{u_i u_j u_k} - \nu\frac{\partial\overline{u_i u_j}}{\partial x_k}\right] \quad (1)$$

where U and u denote the mean and fluctuating components of velocity, respectively, p represents the fluctuation in static pressure about the mean value, ρ is the density, ν is the viscosity, and x denotes Cartesian space coordinates.

The first term in the right-hand side is the shear production term, which is exact at the second-order modeling level. The second term is the dissipation tensor, of which model is decomposed into a deviatoric part and an isotropic one (Lumley 1978):

$$\varepsilon_{ij} = 2\nu\overline{\frac{\partial u_i}{\partial x_k}\frac{\partial u_j}{\partial x_k}} = 2\varepsilon\, d_{ij} + \tfrac{2}{3}\varepsilon\delta_{ij} \quad (2)$$

The deviatoric part $2\varepsilon d_{ij}$, contributes to interchange the turbulent kinetic energy among components, but neither creates nor destroys the total energy.

Pressure strain model

The pressure gradient-velocity correlation term in Equation 1 is generally separated into a deviatoric part Φ_{ij} and a nondeviatoric part T_{ij} as follows:

$$-\frac{1}{\rho}\overline{\left(u_i\frac{\partial p}{\partial x_j} + u_j\frac{\partial p}{\partial x_i}\right)} = \Phi_{ij} + T_{ij} \quad (3)$$

Because the deviatoric part is trace free; i.e., $\Phi_{ii} = 0$, it is interpreted as an intercomponent energy redistribution term in an incompressible flow. The second term T_{ij} represents the spatial transport of the Reynolds stress by the pressure fluctuations.

For the deviatoric part Φ_{ij}, which has been conventionally named the pressure strain term, the following linear model of LRR, which includes the return-to-inotropy model of Rotta (1951), has been widely used in the past:

$$\Phi_{ij} = -C_1\varepsilon b_{ij} - \frac{C_2+8}{11}(P_{ij} - \tfrac{2}{3}P\delta_{ij}) - \frac{8C_2-2}{11}(D_{ij} - \tfrac{2}{3}P\delta_{ij}) - \frac{30C_2-2}{55}\kappa\left(\frac{\partial U_i}{\partial x_j} + \frac{\partial U_j}{\partial x_i}\right) \quad (4)$$

where

$$P_{ij} = -\left(\overline{u_j u_k}\frac{\partial U_i}{\partial x_k} + \overline{u_i u_k}\frac{\partial U_j}{\partial x_k}\right)$$

$$D_{ij} = -\left(\overline{u_i u_k}\frac{\partial U_k}{\partial x_j} + \overline{u_j u_k}\frac{\partial U_k}{\partial x_i}\right)$$

$$P = -\overline{u_i u_k}\frac{\partial U_i}{\partial x_k}$$

The anistotropy tensor b_{ij} is defined as $\overline{u_i u_j}/2\kappa - 1/3\delta_{ij}$, and model constants are $C_1 = 3.0$ and $C_2 = 0.4$. According to Lumley (1978), this model violates the realizability of the 2-D turbulence state. In addition, there is the following nonlinear SSG model of Φ_{ij}, which satisfies the realizability condition of Pope (1985),

$$\Phi_{ij} = C_0\varepsilon b_{ij} + C_1\varepsilon(b_{ik}b_{jk} - 1/3II_b\delta_{ij}) + C_2\kappa S_{ij} + C_3 P b_{ij} + C_4\kappa(b_{ik}S_{jk} + b_{jk}S_{ik} - 2/3\delta_{ij}b_{kl}S_{ll}) + C_5\kappa(b_{ik}W_{jk} + b_{jk}W_{ik}) \quad (5)$$

where

$$S_{ij} = \frac{1}{2}\left(\frac{\partial U_i}{\partial x_i} + \frac{\partial U_j}{\partial x_i}\right)$$

$$W_{ij} = \frac{1}{2}\left(\frac{\partial U_i}{\partial x_i} - \frac{\partial U_j}{\partial x_i}\right)$$

$C_0 = -3.4$; $C_1 = 4.2$; $C_2 = 0.8 - 1.3\Pi_b^{1/2}$; $C_3 = -1.8$; $C_4 = 1.25$; $C_5 = 0.40$; and Π_b is the second invariant of b_{ij} defined as $b_{ik}b_{kl}$.

Pressure transport model

The expressions for the deviatoric part Φ_{ij} and the nondeviatoric part T_{ij} are not unique. There are three different methods of separation to identify Φ_{ij} and T_{ij} in current modeling approach (Groth 1991). A classical separation was given by LRR as follows:

$$\Phi_{ij} = \frac{\overline{p}}{\rho}\overline{\left(\frac{\partial u_i}{\partial x_j} + \frac{\partial u_j}{\partial x_i}\right)}$$

$$T_{ij} = \frac{\partial}{\partial x_n}\left[-\frac{\overline{p}}{\rho}\overline{(u_i\delta_{nj} + u_j\delta_{ni})}\right] \quad (6)$$

Another one is the isotropic pressure transport model suggested by Lumley (1975) as follows:

$$\Phi_{ij} = -\left[\frac{1}{\rho}\overline{\left(u_i\frac{\partial p}{\partial x_j} + u_j\frac{\partial p}{\partial x_i}\right)} - \frac{2}{3\rho}\frac{\partial\overline{pu_n}}{\partial x_n}\delta_{ij}\right]$$

$$T_{ij} = -\frac{2}{3\rho}\frac{\partial\overline{pu_n}}{\partial x_n}\delta_{ij} \quad (7)$$

Finally, the third separation was proposed by Mansour, Kim, and Moin (1988, hereinafter referred to as MKM) in the following way:

$$\Phi_{ij} = -\left[\frac{1}{\rho}\overline{\left(u_i\frac{\partial p}{\partial x_j} + u_j\frac{\partial p}{\partial x_i}\right)} - \frac{\overline{u_i u_j}}{\kappa}\frac{1}{\rho}\frac{\partial\overline{pu_n}}{\partial x_n}\right]$$

$$T_{ij} = -\frac{\overline{u_i u_j}}{\kappa}\frac{1}{\rho}\frac{\partial\overline{pu_n}}{\partial x_n} \quad (8)$$

Because the model for Φ_{ij} is usually formulated as a whole term based on its physical role as the intercomponent energy transfer, there is no difference between separation methods insofar as the model of Φ_{ij} is trace free. Concerning the pressure transport, however, they lead to a decidedly different effect, which has been discussed by Speziale (1985). He investigated the justification of the first two approaches and concluded that only the second approach was consistent with the Navier–Stokes equation in the limit of 2-D turbulence subjected to a high rotation rate.

Using the same analysis method of Speziale (1985), it can be found that MKM's separation is also consistent with the Navier–Stokes equation. Moreover, a physical realizability (Groth 1991) requires that there should be no net work done by the pressure, which otherwise generates energy in the component having zero turbulent energy in the 2-D turbulence.

Lumley's separation does not satisfy this condition; whereas, both the classical and MKM's separations meet this. Therefore, it is concluded the MKM's is the only one that satisfies the above two conditions.

Lumley (1978) modeled the pressure–velocity correlation vector as $-\overline{pu_i}/\rho = (1/5)\overline{u_i u_j u_j}$. This model implies that the pressure transport counterdiffuses the Reynolds stresses against the diffusion by the triple velocity correlation in the Reynolds stress equation.

Quite recently, we developed a new pressure transport model (Kim and Chung 1994). The pressure–velocity correlation vector has been modeled by adopting the concept of a convection velocity for the unsteady term in the inviscid, irrotational momentum equation. The final form is written as follows:

$$-\frac{\overline{pu_i}}{\rho} = C_p[(U_j - U_{cj})\overline{u_i u_j} + \tfrac{1}{2}\overline{u_i u_j u_j}] \tag{8}$$

where the convection velocity U_{cj} is defined as $\partial u_i/\partial t = -U_{cj}\,\partial u_i/\partial x_i$. Furthermore, the convection velocity is estimated in terms of the intensity of turbulence, skewness, and the velocity scale of large-scale eddies by the following form:

$$U_{ci} = U_i - C_{c1}\exp(-C_{c2}I)\frac{\overline{u_j u_n u_n}}{\varepsilon}\frac{\partial U_i}{\partial x_j} \tag{9}$$

where I is the intensity of turbulence defined by $I = \sqrt{\kappa/(U_m U_m)}$, and the model constants are $C_{c1} = 0.28$ and $C_{c2} = 0.6$. The term $\exp(-C_{c2}I)$ in Equation 9, which expresses the degree of coherence of the large-scale structure, goes to zero, which indicates complete incoherence as the turbulence intensity becomes large; e.g., when U_m approaches to zero. When the frame of reference is moving at a constant velocity $\boldsymbol{U}_F$, then the velocity $\boldsymbol{U}$ used in calculation of $\boldsymbol{I}$ must be replaced by $\boldsymbol{U}$-$\boldsymbol{U}_F$ to secure the Galilian invariance of the scalar I. Details of the derivation is given in Kim and Chung (1994). Therefore, the new model of the pressure transport was suggested in the following form:

$$-\frac{\overline{pu_i}}{\rho} = C_p\left[C_{c1}\exp(-C_{c2}I)\frac{\overline{u_1 u_n u_n}}{\varepsilon}\frac{\partial U_j}{\partial x_l}\overline{u_i u_j} + \tfrac{1}{2}\overline{u_i u_j u_j}\right] \tag{10}$$

with $C_p = 0.4$. The two terms of the right-hand side were interpreted as a bulk convective transport term (rapid part) and a turbulent diffusion term (slow part), respectively.

Diffusion model

The triple velocity correlation was approximated by the gradient-type diffusion model by HL as follows:

$$\overline{u_i u_j u_k} = -C_s\frac{\kappa}{\varepsilon}\left(\overline{u_i u_l}\frac{\partial\overline{u_j u_k}}{\partial x_l} + \overline{u_j u_l}\frac{\partial\overline{u_k u_i}}{\partial x_l} + \overline{u_k u_l}\frac{\partial\overline{u_i u_j}}{\partial x_l}\right) \tag{11}$$

where the constant C_s is assigned the value 0.11. Meanwhile, Demuren and Sarkar (1993) recommended the diffusion model of MH written as follows:

$$\overline{u_i u_j u_k} = -C_s'\frac{\kappa^2}{\varepsilon}\left(\frac{\partial\overline{u_i u_j}}{\partial x_k} + \frac{\partial\overline{u_i u_k}}{\partial x_j} + \frac{\partial\overline{u_j u_k}}{\partial x_j}\right) \tag{12}$$

with $C_s' = 2/3C_s$, as a counterpart of the SSG's pressure strain model in their computation of a channel flow. As was pointed out by Schwarz and Bradshaw (1994), the MH model is an isotropic version of the HL model in Equation 11.

Dissipation rate equation

Because nearly all terms in the exact dissipation rate equaiton must be modeled, the main modeling error has been known to arise in the dissipation equation (Launder 1984). A basic form of the dissipation rate equation adopted from HL reads as follows:

$$\frac{d\varepsilon}{dt} = C_\varepsilon\frac{\partial}{\partial x_1}\left(\frac{\kappa}{\varepsilon}\overline{u_l u_m}\frac{\partial\varepsilon}{\partial x_m}\right) - C_{\varepsilon 1}\frac{\varepsilon}{\kappa}\overline{u_l u_m}\frac{\partial U_l}{\partial x_m} - C_{\varepsilon 2}\frac{\varepsilon^2}{\kappa} \tag{13}$$

Investigating the computational anomaly problem between a jet and a wake, Cho and Chung (1992) found that a modification caused by the intermittency must be made to Equation 13.

$$\frac{d\varepsilon}{dt} = C_\varepsilon\frac{\partial}{\partial x_l}\left(\frac{\kappa}{\varepsilon}\overline{u_l u_m}\frac{\partial\varepsilon}{\partial x_m}\right) - C_{\varepsilon 1}\frac{\varepsilon}{\kappa}\overline{u_l u_m}\frac{\partial U_l}{\partial x_m} + \frac{\varepsilon^2}{\kappa}(-C_{\varepsilon 2} + C_{\varepsilon g}\Gamma) \tag{14}$$

where

$$\Gamma = \frac{\kappa^{2.5}}{\varepsilon^2}\frac{U_i}{(U_k U_k)^{0.5}}\frac{\partial U_i}{\partial x_j}\frac{\partial\gamma}{\partial x_j}$$

The quantity Γ proposed by Cho and Chung (1992) is the intermittency interaction invariant term, which represents the entrainment of irrotational fluid into rotational one or vice versa by an interaction between the mean velocity gradient and the intermittency field. The same arguments as I in Equation 9 is necessary about the mean velocity U_k to guarantee the Galilian invariance of scalar Γ. The model constants C_ε, $C_{\varepsilon 1}$, $C_{\varepsilon 2}$ and $C_{\varepsilon g}$ are assigned with the conventional values found in the literature; i.e., $C_\varepsilon = 0.15$(LRR), $C_{\varepsilon 1} = 1.44$(LRR), $C_{\varepsilon 2} = 1.90$(LRR), and $C_{\varepsilon g} = 0.1$ (Cho and Chung 1992).

Intermittency equation

To calculate Γ in Equation 14 an intermittency equation of Cho and Chung (1992) is adopted here. After replacing the eddy–viscosity-type diffusion model with the intermittency diffusion model suggested by Byggstoyl and Kollmann (1986), which is compatible with the Reynolds stress modeling, the intermittency equation takes the following form:

$$\frac{d\gamma}{dt} = C_g\frac{\partial}{\partial x_1}\left[(1-\gamma)\frac{\kappa}{\varepsilon}\overline{u_1 u_m}\frac{\partial\gamma}{\partial x_m}\right] + C_{g1}\gamma(1-\gamma)\frac{P}{\kappa} + C_{g2}\frac{\kappa^2}{\varepsilon}\frac{\partial\gamma}{\partial x_j}\frac{\partial\gamma}{\partial x_j} - C_{g3}\gamma(1-\gamma)\frac{\varepsilon}{\kappa}\Gamma \tag{15}$$

Here, the zone-averaged quantities in the model of Byggstoyl and Kollmann (1986) were approximated by the conventional time means in the present model. The model constant C_g of 0.16 is adopted from Byggstoyl and Kollmann, and the remaining constants C_{g1}, C_{g2}, and C_{g3} are assigned the values 1.60, 0.15, and 0.16, respectively, as in Cho and Chung (1992).

Applications to turbulent free shear flows

Computational method

The Reynolds stress models described in the following section are applied to compute various 2-D free shear flows; namely, a plane mixing layer, a plane jet, and a plane far wake. For these thin boundary–layer-type flows at high Reynolds numbers, the stream-wise momentum equation and the continuity equation are as follows:

$$U\frac{\partial U}{\partial x}+V\frac{\partial U}{\partial y}=-\frac{\partial \overline{uv}}{\partial y}-\frac{\partial}{\partial x}(\overline{u^2}-\overline{v^2}) \quad (16)$$

$$\frac{\partial U}{\partial x}+\frac{\partial V}{\partial y}=0 \quad (17)$$

The upwind finite–difference procedure was used to solve the system of the governing equations (e.g., Patankar 1980). Calculations of the flows reported below were obtained by using 400 cross-stream nodes and a very small marching step to secure the streamwise spatial resolution. To demonstrate the numerical solution accuracy, numerical errors depending upon the number of grids and the downstream increment are presented in Figure 1. The results were obtained in computing a fully developed plane jet flow with stagnant surroundings using the LRR's Reynolds stress model. From Figure 1a, the calculated Reynolds shear stress profiles with 200 and 400 cross-stream nodes are nearly the same. Based upon Figure 1b, the streamwise step size Δx was taken as 2% of the local jet half-width. The same procedure to guarantee the numerical accuracy was processed prior to the computation of each flow. The initial boundary layers for all flows were assumed to be in a fully developed turbulent state, having the initial profiles similar to that in Klebanoff's experiment (Hinze 1975). The initial dissipation rate profiles were estimated by assuming a local equilibrium.

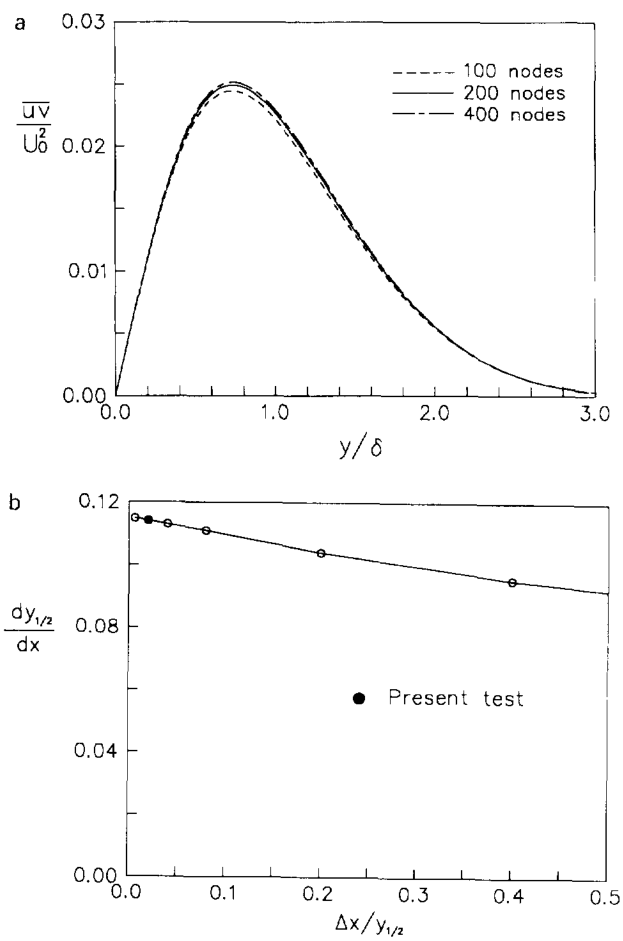

Figure 1 Numerical solution errors in calculating a turbulent plane jet with the model of Launder, Reece, and Rodi (1975): a. Variation of calculated Reynolds stress profiles with the number of cross-stream nodes; b. Variation of calculated spreading rates with streamwise step size

Model set alternatives

First, two diffusion models, Equations 11 and 12, and the pressure strain models, Equations 4 and 5, have been tested in free shear flows in order to construct a best basic reference set of the Reynolds stress model. The conventional LRR's Reynolds stress model, which includes the HL's diffusion model and LRR's pressure strain model, is compared with the MSS model (MH's diffusion model and SSG's pressure strain model) and the HSS model (HL's diffusion model and SSG's pressure strain model). Although LRR's pressure strain model is incompatible with the present pressure transport model in the sense that it does not satisfy the realizability condition, LRR's model is included in this comparison because of its popularity. Figures 2a, b, and c show the comparisons of the model predictions with experimental Reynolds stress distributions in a plane mixing layer, a plane jet and a plane far wake. Two kinds of HSS model with different model constants are presented here. The HSS1 model has the same $C_{\varepsilon 1}$ and $C_{\varepsilon 2}$ as those of LRR, but the HSS2 model has constants modified to adjust the level of Reynolds shear stress in a plane mixing layer. Table 1 shows the construction of various Reynolds stress model sets. It is clearly seen that the MH's diffusion model is not compatible for the computation of free shear flows. From Figure 2c, all models are found to underpredict severely the level of the Reynolds shear stress of a plane far wake.

In the following sections, the computations are performed with four different sets of models. The first and second sets are LRR and HSS2, both of which have almost the same Reynolds shear stresses, which are better than those of the remaining ones. However, because HSS2 adopted more recent pressure strain model of SSG, it is selected as the basic Reynolds stress model to formulate the model sets PM1 and PM2, which follow. The difference between the results of LRR and HSS2 will isolate the performance of the pressure strain models of LRR and SSG. The third one is constructed by replacing the dissipation rate equation of LRR with Equation (14). The intermittency Equation 15 is included here, of course. This model set is identified by PM1. As a last model set, the pressure transport model of Kim and Chung (1994) is included in the model set PM1. For this model set PM2, the model constant C_s in Equation (11) should be modified, because the conventional diffusion models such as Equation 11 had been adjusted without the pressure transport term; whereas, the present pressure transport model includes the same third-order moment as the counter diffusion term as appeared in Equation (10). Considering this counterdiffusion effect of the pressure transport, the constant C_s was determined to be 0.13 instead of LRR's value of 0.11. The computational results by this third model set PM2 will provide a concrete ground to judge the justification of the pressure transport model.

Note that all terms in the reference Reynolds stress equation and the dissipation equatin are retained in PM1 and PM2: the streamwise diffusion terms and the secondary production terms which are related to the streamwise gradient are all included. The secondary source terms in the Reynolds stress equation and the dissipation equation have non-negligible effect in computation of free shear flows (Launder and Morse 1979; Hanjalic and Launder 1980).

In the following figures, because the predicted profiles by both models LRR and HSS2 are more or less the same, the profiles obtained by HSS2 are presented for clarity of comparison to those of PM1 and PM2.

Plane mixing layer

In Figures 3a–c, the computational results for the plane mixing layer with the velocity ratio of $R = 0.6$, are compared with

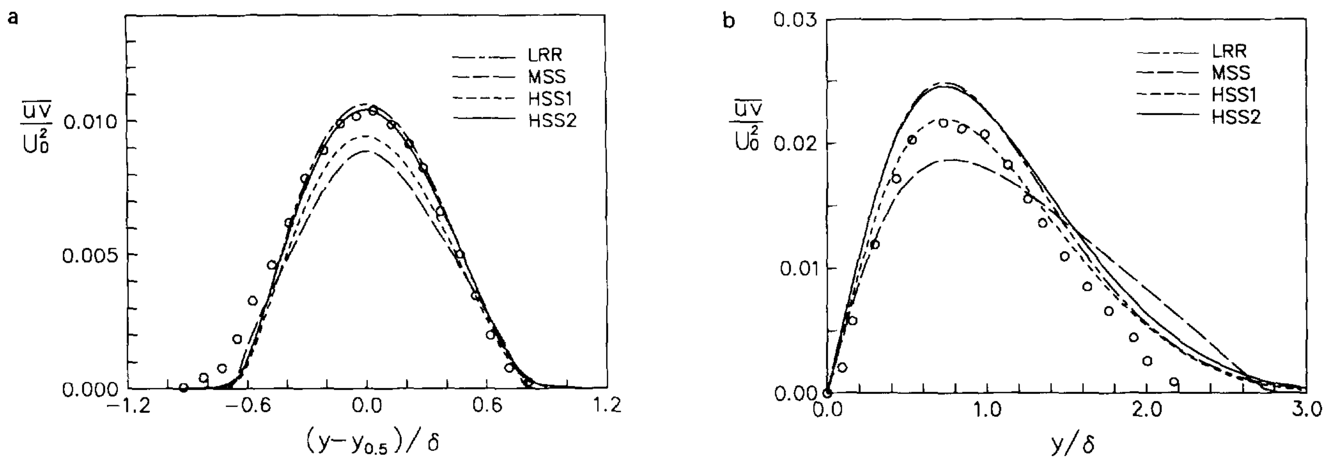
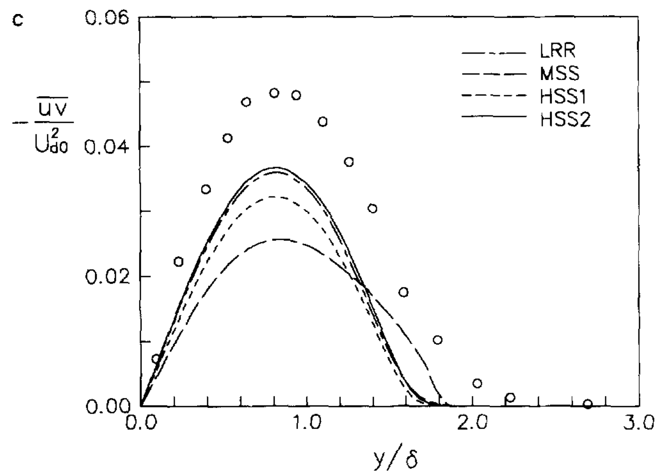

Figure 2 Predicted Reynolds shear stresses and the experiments for a plane mixing layer with $R = 0.6$, the self-preserving region of a plane jet with stagnant surroundings and a plane far wake: a. Plane mixing layer with $R = 0.6$ (circles denote experimental data of Bell and Metha 1990); b. Self-preserving region of a plane jet with stagnant surroundings (circles denote experimental data of Heskestad 1965); c. Plane far wake (circles denote experimental data of Wygnanski, Champagne, and Marasli 1986)

available experimental data. Here, R is the ratio of the lower freestream speed U_L to the higher one U_H. The plane mixing layer is experimentally generated with two parallel freestreams with a separating flat-plate between them. The initial development zone of a plane jet is one of the plane mixing layer flows. In these figures, U_0 represents the velocity difference, $U_H - U_L$, the shear layer thickness δ is defined by the distance $|y_{0.1} - y_{0.9}|$, and $y_{0.1}$, $y_{0.5}$ and $y_{0.9}$ indicate cross-stream locations where $U - U_L$ is 10%, 50%, and 90% of U_0, respectively.

The predictions are compared in Figures 3a–c together with the data of Bell and Metha (1990). For the mean flow profile, the inclusion of the intermittency term is most critical for the improvement in the prediction. On comparing the various model predictions for the Reynolds stresses, it is apparent that both the intermittency and the pressure transport models contribute favorably to the improvement of the prediction accuracy. Especially, in the high velocity side, all the Reynolds shear and normal stresses are significantly better predicted by including both flow mechanisms in the computations. However, the Reynolds normal stresses are somewhat underestimated by both PM1 and PM2 model sets in the low velocity side. In the 1980–81 Stanford Conference, Birch (1982) recommended a spreading rate relation of $dL/dx = 0.115(1 - R)/(1 + R)$ after surveying experimental data. Here, L is the distance between the points where $U = \sqrt{0.9}(U_H -$

Table 1 Comparative model sets

Model set	Reynolds stress equation: Diffusion	Reynolds stress equation: Pressure strain	Reynolds stress equation: Pressure transport	Disspiation equation: $C_{\varepsilon 1}$	Disspiation equation: $C_{\varepsilon 2}$	Intermittency equation
LRR	HL	LRR	—	1.45	1.90	—
MSS	MH	SSG	—	1.45	1.90	—
HSS1	HL	SSG	—	1.45	1.90	—
HSS2	HL	SSG	—	1.40	1.92	—
PM1	HL	SSG	—	1.40	1.92	Cho and Chung (1992)
PM2	HL ($C_s = 0.13$)	SSG	Kim and Chung (1994)	1.40	1.92	Cho and Chung (1992)

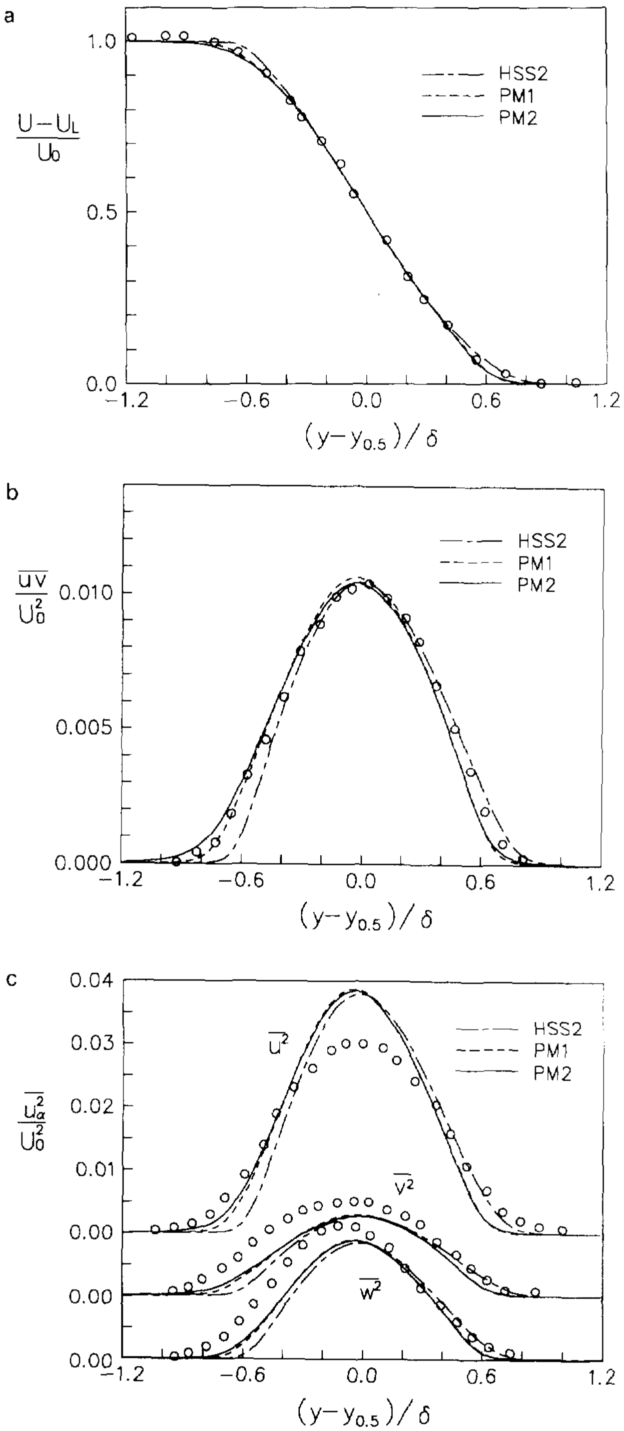

Figure 3 Comparisons of prediction with the experiments for a plane mixing layer with $R = 0.6$ (circles denote experimental data of bell and Metha 1990): a. Streamwise mean velocity profiles; b. Reynolds shear stress profiles; c. Profiles of the normal components of the Reynolds stresses

$U_L) + U_L$, and $U = \sqrt{0.1}(U_H - U_L) + U_L$. According to this relation, dL/dx is 0.029 in the case of $R = 0.6$. LRR, HSS2, and PM1 predict the spreading rate to be 0.027, 0.027, and 0.031, respectively. However, the final model PM2 yields the correct rate of 0.029.

Figure 4 shows the turbulent kinetic energy balanfe budgets calculated by PM2 and DNS data of Rogers and Moser (1994).

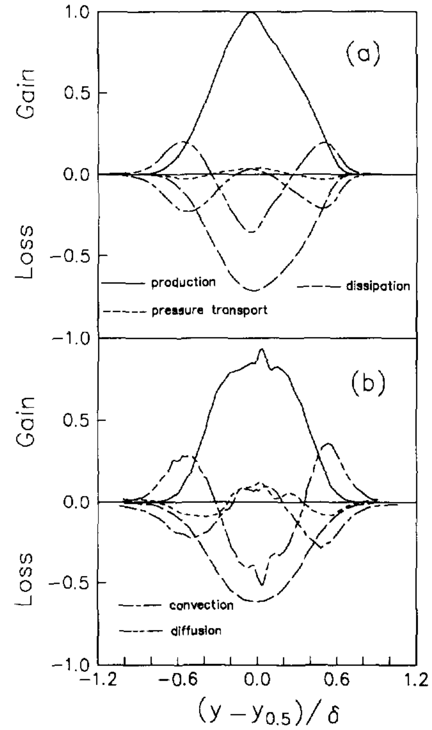

Figure 4 the comparison of turbulent kinetic energy budgets for a plane mixing layer; a. Prediction by the model set PM2; b. DNS data of Rogers and Moser 1994

Each term presented in this figure is the normalized one by the cube of the characteristic velocity scale U_0, divided by the length scale δ, and multiplied by 100. Both the production and the dissipation terms are the main balancing quantities in the turbulent kinetic energy. It is seen that the contribution of the pressure transport term evaluated by the present model is somewhat small, as compared to the DNS data. It is noted that the computed diffusion term by the triple velocity correlation is reasonably well compared with DNS data in Figure 4b.

Plane jet

The computational results for a plane jet into a stagnant surroundings are compared with the hot-wire data of Heskestad (1965) in Figures 5a–c. The shear layer thickness δ defined by the distance $y_{0.5}$, and U_0 is the centerline mean velocity. The predicted mean velocity profile by PM2 agrees best with the experimental data in Figure 5a. For the Reynolds shear stress profiles in Figure 5b, both models PM1 and PM2 yield good results. However, for the Reynolds normal stresses, HSS2 shows a little better prediction than PM1 and PM2. For the spreading rate, $d\delta/dx$, Rodi (1975) suggested a value 0.11, but Haworth and Pope (1987) recommended a value of 0.10.

PM1 and PM2 yielded the spreading rate as 0.101, but LRR and HSS2 overpredicted it as 0.114. The better results of PM1 over HSS2 are attributable to the intermittency model, which increases the dissipation, and thus, decreases the Reynolds stresses. The notable difference of the results between PM1 and PM2 appearing in the free boundary region especially for the Reynolds shear stress is caused by the pressure transport term.

Plane far wake

Figures 6a–c represent the computational results for a plane far wake, as compared to experimental data. It is well known (see Wygnanski, Champagne, and Marasli (1986) that the flow field

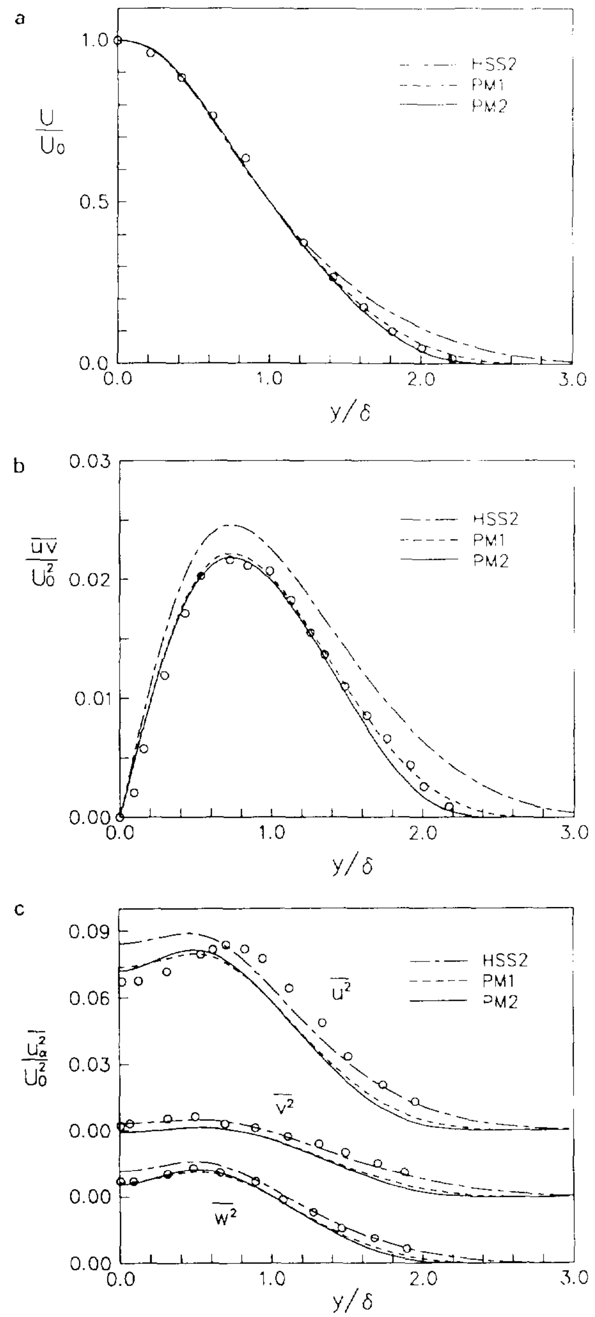

Figure 5 Comparisons of predictions with the experiments for the self-preserving region of a plane jet with stagnant surroundings (circles denote experimental data of Hessskestad 1965): a. Streamwise mean velocity profiles; b. Reynolds shear stress profiles; c. Profiles of the normal components of the Reynolds stresses

in the plane far wake depends largely upon the wake generator. Because reliable experimental data set for the plane far wake behind a flat plate are scarce, a data set for the plane far wake behind a symmetric airfoil of Wygnanski, Champagne, and Marasli was chosen as the comparative data. Here, U_∞ is the freestream velocity, U_d is the defect velocity defined by the difference, $U_\infty - U$, U_{d_0} denotes its center-line value, and the shear layer thickness δ is the distance $y_{0.5}$. The calculated mean defect velocity profile with HSS2 in Figure 6a shows very poor agreement with the data near the free-stream edge. As was expected, PM1 makes much improvement in that region where the intermittency model plays an important role. PM2 gives a nearly identical profile with the mean defect velocity data. Apparently, the improvement is made by the pressure transport model.

The spreading rates $d(0.5U_\infty y_{0.5}/U_{d0})/dx$ defined by Rodi (1975) were calculated to be 0.070, 0.071, 0.107, and 0.100 with LRR, HSS2, PM1, and PM2, respectively. Comparing these values with the value of 0.098, which was recommended at the Stanford conference in 1982, LRR and HSS2 yield significantly too low values, and only the model PM2 produces the nearly exact spreading rate. The experimental decay rate of the centerline defect velocity, $U_d x/(U_\infty \theta)$, defined by Wygnanski, Champagne, and Marasli (1986), varies in a range 1.56–1.71 when the wake generator is flat plates or symmetric airfoils.

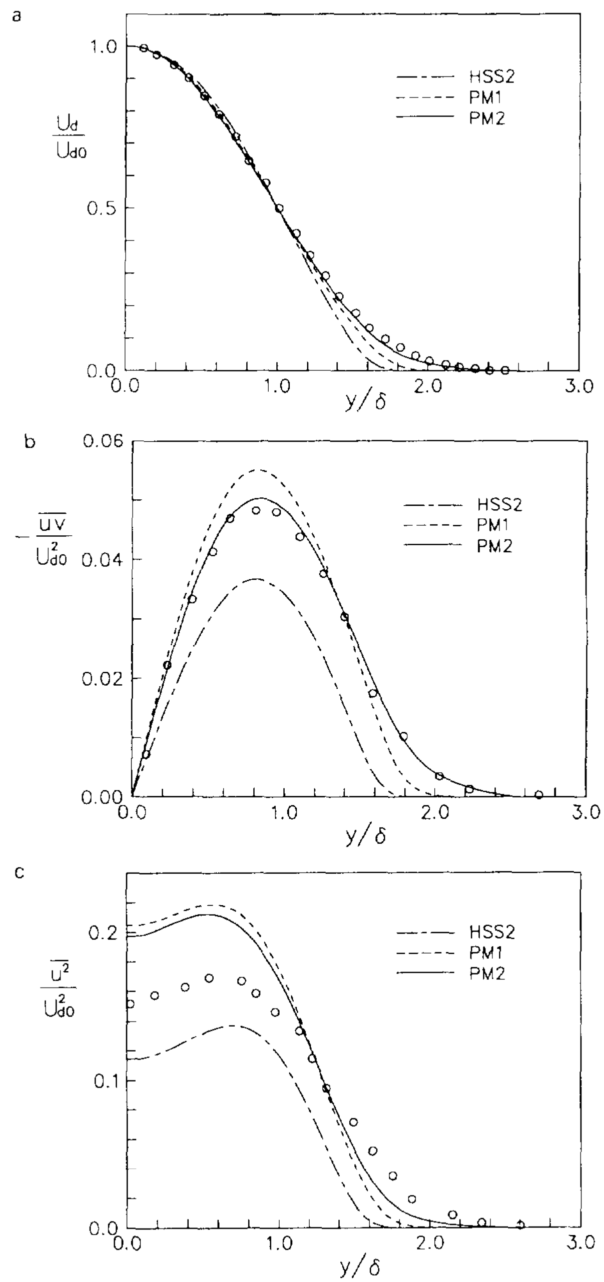

Figure 6 Comparisons of predictions with the experiments for a plane far wake (circles denote experimental data of Wygnanski, Champagne, and Marasli 1986): a. Streamwise mean defect velocity profiles; b. Reynolds shear stress profiles; c. Profile of the streamwise normal stress

Here, θ stands for the momentum thickness. Although PM1 and PM2 predict the decay rate as 1.51 amd 1.58, respectively, both LRR and HSS2 overpredict it by as high as 1.82. Such an improvement by PM1 and PM2 is obtained mainly from the intermittency interaction model. In Figures 6b and c, the Reynolds shear and normal stresses are predicted too low by about 20–40% by LRR and HSS2 models. The inclusion of the intermittency model remarkably improves the prediction accuracy for the Reynolds shear stress. In the central and outer regions, the improvement by the pressure transport model for the Reynolds shear stress in Figure 6b is quite apparent. However, the stream-wise turbulent intensity $\overline{u^2}$ in Figure 6c is a little overestimated by the present models, although it is better predicted in the outer region by the inclusion of the intermittency term and the pressure term. More data for $\overline{v^2}$ and $\overline{w^2}$ are needed to evaluate the model performance in the central region.

Concluding remarks

The pressure transport model of Kim and Chung 1994 and the intermittency model of Cho and Chung (1992) have been tested against various free shear flows. The conventional Reynolds stress model of Launder, Reece, and Rodi (1975) was modified to construct three different sets of Reynolds stress closure. The variants were made by including the pressure strain model of Speziale, Sarkar, and Gatski (1991), the intermitency interaction model and the pressure transport model into the basic form of LRR model. The SSG's pressure strain model affected the computational results; however, any merit of this model over the LRR model was not detected in these computations.

It was found that the intermittency interaction model of Cho and Chung (1992) contribute greatly to the improvement of the predictions of all flows considered here. The favorable role of the intermittency in remedying the plane jet/plane wake anomaly problem that has been shown by Cho and Chung (1992) at the level of k–ε model was also confirmed at the Reynolds stress closure level.

Fairly good role of the present pressure transport model in improving the predictions were clearly seen in the freestream edges of all free shear flows treated here. specifically, the increase in the Reynolds stresses by the dominant bulk convective pressure transport much improved the prediction accuracy in the high-velocity side of the plane mixing layer and the outer layer of the plane far wake. Therefore, it can be concluded that the combined role of the intermittency interaction and the pressure transport is very important in computing the free shear flows.

However, it should be noted that the present final model set PM2, which includes both the intermittency and the pressure transport models, do not predict well the Reynolds normal stresses, whereas it improves the Reynolds shear stress remarkably. This suggests that further improvements are needed in the model of the intercomponent energy redistribution term by the pressure fluctuations.

References

Bell, J. H. and Metha, R. D. 1990. Development of a two-stream mixing layer from tripped and untripped boundary layers. *AIAA J*, **28**, 2034–2042

Birch, S. 1982. Planar mixing layer. In *Proc. 1980–81 AFOSR-HTTM-Stanford Conference on Complex Turbulent Flows*, Kline et al. (eds.). Stanford Univ., Stanford, 170

Bradshaw, P. 1994. Turbulence: The chief outstanding difficulty of our subject. *Exp. Fluids*, **16**, 203–216

Byggstoyl, S. and Kollmann, W. 1986. A closure model for conditioned stress equations and its application to turbulent shear flows. *Phys. Fluids*, **29**, 1430–1440

Cho, J. R. and Chung, M. K. 1992. A k-ε-γ equation turbulence model. *J. Fluid Mech.*, **237**, 301–322

Demuren, A. O. and Sarkar, S. 1993. Perspective: Systematic study of Reynolds stress closure models in the computations of plane channel flows. *J. Fluids Eng.*, **115**, 5–12

Fu, S., Launder, B. E. and Tselepidakis, D. P. 1987. Accommodating the effects of high strain rates in modeling the pressure–strain correlation. UMIST Mechanical Engineering Dept. Rept. TFD/87/5

Groth, J. 1991. Description of the pressure effects in the Reynolds stress transport equations. *Phys. Fluids A: Fluid Dyn.*, **3**, 2276–2277

Hanjalic, K. and Launder, B. E. 1972. A Reynolds stress model of turbulence and its application to thin shear flows. *J. Fluid Mech.*, **52**, 609–638

Hanjalic, K. and Launder, B. E. 1980. Sensitizing the dissipation equation to irrotational strains. *J. Fluids Eng.*, **102**, 34–40

Haworth, D. C. and Pope, S. B. 1986. A generalized Langevin model for turbulent flows. *Phys. Fluids*, **29**, 387–405

Haworth, D. C. and Pope, S. B. 1987. A pdf modeling study of self-similar turbulent-free shear flows. *Phys. Fluids*, **30**, 1026–1044

Heskestad, G. 1965. Hot-wire measurements in a plane turbulent jet. *J. Appl. Mech.*, **32**, 721–734

Hinze, J. O. 1975. *Turbulence*, 2nd ed., McGraw Hill, New York

Kim, S. K. and Chung, M. K. 1994. Spatial transport of Reynolds stresses by pressure fluctuations. *Phys. Fluids*, **6**, 3507–3509

Launder, B. E. 1984. Progress and prospects in phenomenological turbulence models. In *Theoretical Approaches to Turbulence*, Dwoyer et al. (eds.), Springer, New York, 155–186

Launder, B. E. and Morse, A. P. 1979. Numerical prediction of axisymmetric free shear flows with a Reynolds stress closure. In *Turbulent Shear Flows* 1, F. Durst et al. (eds.) Springer, New York, 179–294

Launder, B. E., Reece, G. J. and Rodi, W. 1975. Progress in the development of a Reynolds-stress turbulence closure. *J. Fluid Mech.*, **68**, 538–566

Lumley, J. L. 1975. Pressure-strain correlation. *Phys. Fluids*, **18**, 750

Lumley, J. L. 1978. Computational modeling of turbulent flows. *Advances in Applied Mechanics*, vol. **18**, Academic, San Diego, 123–176

Mansour, N. N., Kim, J. and Moin, P. 1988. Reynolds-stress and dissipation-rate budgets in a turbulent channel flow. *J. Fluid Mech.*, **194**, 15–44

Mellor, G. L. and Herring, H. J. 1973. A survey of the mean turbulent field closure models. *AIAA J.*, **11**, 590–599

Patankar, S. V. 1980. Numerical heat transfer and fluid flow. McGraw Hill, New York, 83

Pope, S. B. 1985. Pdf methods for turbulent reactive flows. *Prog. Energy Combust. Sci.*, **11**, 119–192

Rodi, W. 1975. A review of experimental data of uniform density free turbulen layers. In *Studies in Convection*, Launder, B. E. (ed.), Academic Press, London, 79–165

Rogers, M. M. and Moser, R. D. 1994. Direct simulation of a self-similar turbulent layers. *Phys. Fluids*, **6**, 903

Rotta, J. C. 1951. Statistische theorie nichthomogener turbulenze, I. Mitteilung. *Zeitschrift für Physik*, **129**, 547–572

Schwarz, W. R. and Bradshaw, P. 1994. Term-by-term tests of stress-transport turbulence models in a three-dimensional boundary layer. *Phys. Fluids*, **6**, 986–998

Shih, T.-H. and Lumley, J. L. 1985. Modeling of pressure correlation terms in Reynolds stress and scalar flux equations. Sibley School of Mechanical and Aeronautical Engineering, Cornell University, Rept. FDA-85-3, Ithaca, NY, 1985

Shih, T. M., Mansour, N. N. and Chen, J. Y. 1987. Reynolds stress modeling of homogeneous turbulence and comparison with numerical simulation. In *Proc. Summer Program* 1987, *Center for Turbulent Research* (NASA/Ames–Stanford University, Stanford, CA), 191

Speziale, C. G. 1985. Modeling the pressure gradient-velocity correlation of turbulence. *Phys. Fluids*, **28**, 69–71

Speziale, C. G., Sarkar, S. and Gatski, T. B. 1991. Modeling the pressure-strain correlation of turbulence: an invariant dynamic systems approach. *J. Fluid Mech.*, **227**, 245–272

Wygnanski, I., Champagne, F. and Marasli, B. 1986. On the large-scale structures in two-dimensional, small-deficit, turbulent wakes. *J. Fluid Mech.*, **168**, 31–71